Evidence for granularity, anisotropy and lattice distortions in cuprate superconductors and their implications

H. Keller[1] and T. Schneider[1]

[1] *Physik-Institut der Universität Zürich, Winterthurerstrasse 190, CH-8057, Switzerland*

Granularity, anisotropy, local lattice distortions and their dependence on dopant concentration appear to be present in all cuprate superconductors, interwoven with the microscopic mechanisms responsible for superconductivity. Here we review anisotropy and penetration depth measurements to reassess the evidence for granularity, as revealed by the notorious rounded phase transition, the evidence for the three dimensional nature of superconductivity, uncovered by the doping dependence of transition temperature and anisotropy, and to reassess the relevance of the electron-lattice coupling, emerging from the oxygen isotope effects.

To appear in the proceedings of Symmetry and Heterogeneity in High Temperature Superconductors, Erice-Sicily: 4-10 October 2003

Establishing and understanding the phase diagram of cuprate superconductors in the temperature - dopant concentration plane is one of the major challenges in condensed matter physics. Superconductivity is derived from the insulating and antiferromagnetic parent compounds by partial substitution of ions or by adding or removing oxygen. For instance La_2CuO_4 can be doped either by alkaline earth ions or oxygen to exhibit superconductivity. The empirical phase diagram of $La_{2-x}Sr_xCuO_4$ [1, 2, 3, 4, 5, 6, 7, 8, 9] depicted in Fig.1a shows that after passing the so called underdoped limit ($x_u \approx 0.05$), T_c reaches its maximum value $T_c(x_m)$ at $x_m \approx 0.16$. With further increase of x, T_c decreases and finally vanishes in the overdoped limit $x_o \approx 0.27$. This phase transition line is thought to be a generic property of cuprate superconductors [10] and is well described by the empirical relation

$$T_c(x) = T_c(x_m)\left(1 - 2\left(\frac{x}{x_m} - 1\right)^2\right) = \frac{2T_c(x_m)}{x_m^2}(x - x_u)(x_o - x), \qquad (1)$$

proposed by Presland *et al.*[11]. Approaching the endpoints along the x-axis, $La_{2-x}Sr_xCuO_4$ undergoes at zero temperature doping tuned quantum phase transitions. As their nature is concerned, resistivity measurements reveal a quantum superconductor to insulator (QSI) transition in the underdoped limit[12, 13, 14, 15, 16, 17, 18] and in the overdoped limit a quantum superconductor to normal state (QSN) transition[12].

Another essential experimental fact is the doping dependence of the anisotropy. In tetragonal cuprates it is defined as the ratio $\gamma = \xi_{ab}/\xi_c$ of the correlation lengths parallel (ξ_{ab}) and perpendicular (ξ_c) to CuO_2 layers (ab-planes). In

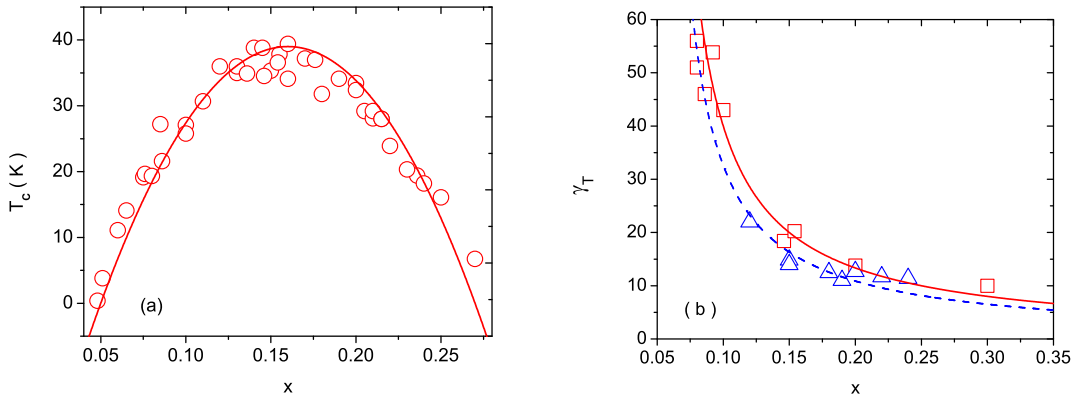

FIG. 1: (a) Variation of T_c for $La_{2-x}Sr_xCuO_4$. Experimental data taken from [1, 2, 3, 4, 5, 6, 7, 8, 9]. The solid line is Eq.(1) with $T_c(x_m) = 39$K. (b) γ_T versus x for $La_{2-x}Sr_xCuO_4$. The squares are the experimental data for γ_{T_c} [1, 2, 4, 6, 7] and the triangles for $\gamma_{T=0}$ [8, 9]. The solid curve and dashed lines are Eq.(2) with $\gamma_{T_c,0} = 2$ and $\gamma_{T=0,0} = 1.63$.

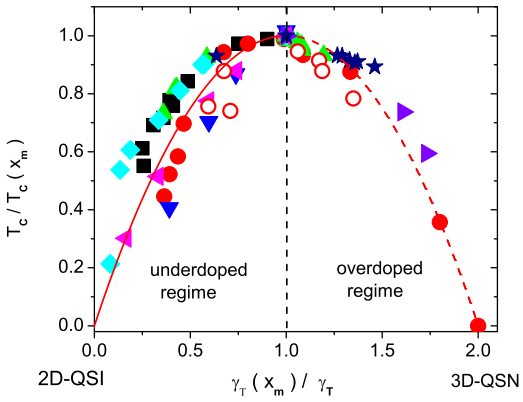

FIG. 2: $T_c(x)/T_c(x_m)$ versus $\gamma_T(x_m)/\gamma_T(x)$ for various cuprate families: $La_{2-x}Sr_xCuO_4$ (•, $T_c(x_m) = 37$K, $\gamma_{T_c}(x_m) = 20$) [1, 2, 4, 6, 7] , (◯, $T_c(x_m) = 37$K, $\gamma_{T=0}(x_m) = 14.9$) [8, 9], $HgBa_2CuO_{4+\delta}$ (▲, $T_c(x_m) = 95.6$K, $\gamma_{T_c}(x_m) = 27$) [20], $Bi_2Sr_2CaCu_2O_{8+\delta}$ (★, $T_c(x_m) = 84.2$K, $\gamma_{T_c}(x_m) = 133$) [23], $YBa_2Cu_3O_{7-\delta}$ (♦, $T_c(x_m) = 92.9$K, $\gamma_{T_c}(x_m) = 8$) [24], $YBa_2(Cu_{1-y}Fe_y)_3O_{7-\delta}$ (■, $T_c(x_m) = 92.5$K, $\gamma_{T_c}(x_m) = 9$)[25], $Y_{1-y}Pr_yBa_2Cu_3O_{7-\delta}$ (▼, $T_c(x_m) = 91$K, $\gamma_{T_c}(x_m) = 9.3$)[26], $BiSr_2Ca_{1-y}Pr_yCu_2O_8$ (◄, $T_c(x_m) = 85.4$K, $\gamma_{T=0}(x_m) = 94.3$)[27] and $YBa_2(Cu_{1-y}\ Zn_y)_3O_{7-\delta}$ (►, $T_c(x_m) = 92.5$K, $\gamma_{T=0}(x_m) = 9$)[28]. The solid and dashed curves are Eq.(3), marking the flow from the maximum T_c to QSI and QSN criticality, respectively.

the superconducting state it can also be expressed as the ratio $\gamma = \lambda_c/\lambda_{ab}$ of the London penetration depths due to supercurrents flowing perpendicular (λ_c) and parallel (λ_{ab}) to the ab-planes. Approaching a nonsuperconductor to superconductor transition ξ diverges, while in a superconductor to nonsuperconductor transition λ tends to infinity. In both cases, however, γ remains finite as long as the system exhibits anisotropic but genuine 3D behavior. There are two limiting cases: $\gamma = 1$ characterizes isotropic 3D- and $\gamma = \infty$ 2D-critical behavior. An instructive model where γ can be varied continuously is the anisotropic 2D Ising model[19]. When the coupling in the y direction goes to zero, $\gamma = \xi_x/\xi_y$ becomes infinite, the model reduces to the 1D case, and T_c vanishes. In the Ginzburg-Landau description of layered superconductors the anisotropy is related to the interlayer coupling. The weaker this coupling is, the larger γ is. The limit $\gamma = \infty$ is attained when the bulk superconductor corresponds to a stack of independent slabs of thickness d_s. With respect to experimental work, a considerable amount of data is available on the chemical composition dependence of γ. At T_c it can be inferred from resistivity ($\gamma = \xi_{ab}/\xi_c = \sqrt{\rho_{ab}/\rho_c}$) and magnetic torque measurements, while in the superconducting state it follows from magnetic torque and penetration depth ($\gamma = \lambda_c/\lambda_{ab}$) data. In Fig. 1b we displayed the doping dependence of $1/\gamma_T$ evaluated at T_c (γ_{T_c}) and $T = 0$ ($\gamma_{T=0}$). As the dopant concentration is reduced, γ_{T_c} and $\gamma_{T=0}$ increase systematically, and tend to diverge in the underdoped limit. Thus the temperature range where superconductivity occurs shrinks in the underdoped regime with increasing anisotropy. This competition between anisotropy and superconductivity raises serious doubts whether 2D mechanisms and models, corresponding to the limit $\gamma_T = \infty$, can explain the essential observations of superconductivity in the cuprates. From Fig. 1b it is also seen that $\gamma_T(x)$ is well described by

$$\gamma_T(x) = \frac{\gamma_{T,0}}{x - x_u}, \tag{2}$$

where $\gamma_{T,0}$ is the quantum critical amplitude. Having also other cuprate families in mind, it is convenient to express the dopant concentration in terms of T_c. From Eqs.(1) and(2) we obtain the correlation between T_c and γ_T:

$$\frac{T_c(x)}{T_c(x_m)} = 1 - \left(\frac{\gamma_T(x_m)}{\gamma_T(x)} - 1\right)^2, \quad \gamma_T(x_m) = \frac{\gamma_{T,0}}{x_m - x_u} \tag{3}$$

Provided that this empirical correlation is not merely an artefact of $La_{2-x}Sr_xCuO_4$, it gives a universal perspective on the interplay of anisotropy and superconductivity, among the families of cuprates, characterized by $T_c(x_m)$ and $\gamma_T(x_m)$. For this reason it is essential to explore its generic validity. In practice, however, there are only a few additional compounds, including $HgBa_2CuO_{4+\delta}$[20], for which the dopant concentration can be varied continuously throughout the entire doping range. It is well established, however, that the substitution of magnetic and nonmagnetic impurities depresses T_c of cuprate superconductors very effectively[21, 22]. To compare the doping and substitution

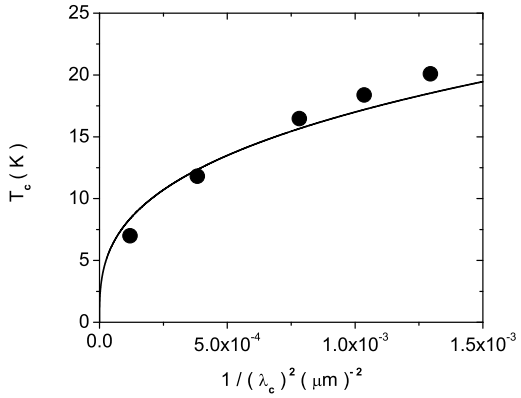

FIG. 3: T_c versus $1/\lambda_c^2(T=0)$ for heavily underdoped $YBa_2Cu_3O_{7-\delta}$ single crystals, taken from Hosseini[35]. The solid line is $T_c = 170\left(1/\lambda_c^2(T=0)\right)^{1/3}$ and indicates the consistency with the 2D-QSI scaling relation $T_c \propto \left(1/\lambda_c^2(0)\right)^{z/(z+2)}$ and $z=1$.

driven variations of the anisotropy, we depicted in Fig. 2 the plot $T_c(x)/T_c(x_m)$ versus $\gamma_T(x_m)/\gamma_T(x)$ for a variety of cuprate families. The collapse of the data on the parabola, which is the empirical relation (3), reveals that this scaling form appears to be universal. Thus, given a family of cuprate superconductors, characterized by $T_c(x_m)$ and $\gamma_T(x_m)$, it gives a universal perspective on the interplay between anisotropy and superconductivity.

Close to 2D-QSI criticality various properties are not independent but related by[13, 14, 15, 16, 17, 18]

$$T_c = \frac{\Phi_0^2 R_2}{16\pi^3 k_B}\frac{d_s}{\lambda_{ab}^2(0)} \propto \gamma_T^{-z} \propto \delta^{z\overline{\nu}}, \tag{4}$$

where k_B is the Boltzmann constant, and Φ_0 the elementary flux quantum. $\lambda_{ab}(0)$ is the zero temperature in-plane penetration depth, z is the dynamic critical exponent, d_s the thickness of the sheets, and $\overline{\nu}$ the correlation length critical exponent of the 2D-QSI transitions. δ measures the distance from the critical point along the x axis (see Fig.1a, and R_2 is a universal number. Since $T_c \propto d_s/\lambda_{ab}^2(0) \propto n_s^{\square}$, where $n_s^{\square}$ is the aerial superfluid density, is a characteristic 2D property, it also applies to the onset of superfluidity in ^{4}He films adsorbed on disordered substrates, where it is well confirmed[29]. A great deal of experimental work has also been done in cuprates on the so called Uemura plot, revealing an empirical correlation between T_c and $d_s/\lambda_{ab}^2(0)$[30]. Approaching 2D-QSI criticality, the data of a given family tends to fall on a straight line, consistent with Eq.(4). Differences in the slope reflect the family dependent value of d_s, the thickness of the sheets, becoming independent in the 2D limit[14, 15, 16, 17, 18]. The relevance of d_s was also confirmed in terms of the relationship between the isotope effect on T_c and $1/\lambda_{ab}^2$[16, 31]. Moreover, together with the scaling form (4) the empirical relation (1) implies 2D-QSI and 3D-QSN transitions with $z=1$, while the empirical relation for the anisotropy (Eqs.(2) and (3)), require $\overline{\nu}=1$ at the 2D-QSI critical point. Thus, the empirical correlations point to a 2D-QSI transition with $z=1$ and $\overline{\nu}=1$.These estimates coincide with the theoretical prediction for a 2D disordered bosonic system with long-range Coulomb interactions, where $z=1$ and $\overline{\nu} \simeq 1$[32, 33, 34]. Here the loss of superfluidity is due to the localization of the pairs, which ultimately drives the transition. From the scaling relation (4) it is seen that measurements of the out of plane penetration depth of sufficiently underdoped systems allow to estimate the dynamic critical exponent z directly, in terms of $T_c \propto \left(1/\lambda_c^2(0)\right)^{z/(z+2)}$, which follows from Eq.(4) with $\gamma_T = \lambda_c(0)/\lambda_{ab}(0)$. In Fig.3 we displayed the data of Hosseini[35] for heavily underdoped $YBa_2Cu_3O_{7-\delta}$ single crystals. The solid line is $T_c = 170\left(1/\lambda_c^2(T=0)\right)^{1/3}$ and uncovers the consistency with the 2D-QSI scaling relation $T_c \propto \left(1/\lambda_c^2(0)\right)^{z/(z+2)}$ with $z=1$.

We have seen that the doping tuned flow to the 2D-QSI critical point is associated with a depression of T_c and an enhancement of γ_T. It implies that whenever a QSI transition is approached, a no vanishing T_c is inevitably associated with an anisotropic but 3D condensation mechanism, because γ_T is finite for $T_c > 0$ (see Figs.1b and 2). This represents a serious problem for 2D models[36] as candidates to explain superconductivity in the cuprates, and serves as a constraint on future work toward a complete understanding. Note that the vast majority of theoretical models focus on a single Cu-O plane, i.e., on the limit of zero intracell and intercell c-axis coupling.

Since Eq.(4) is universal, it also implies that the changes ΔT_c, Δd_s and $\Delta\left(1/\lambda_{ab}^2(T=0)\right)$, induced by pressure or

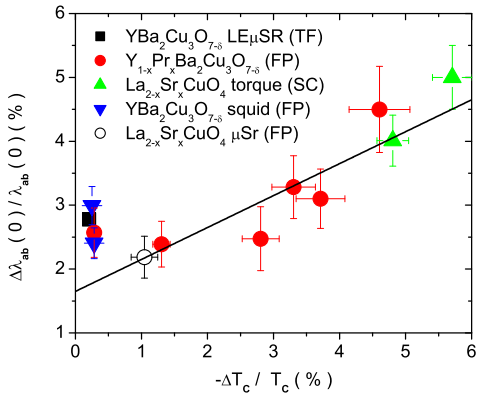

FIG. 4: Data for the oxygen isotope effect in underdoped $La_{2-x}Sr_xCuO_4$(◯: x=0.15[38], ▲:x=0.08, 0.086 [37], $Y_{1-x}Pr_xBa_2Cu_3O_{7-\delta}$ (•: x=0, 0.2, 0.3, 0.4)[38, 39, 40] and $YBa_2Cu_3O_{7-\delta}$ (▼ [38], ■[41]) in terms of $\Delta\left(\lambda_{ab}\left(0\right)\right)/\ \lambda_{ab}\left(0\right)$ versus -$\Delta T_c/T_c$. The solid line indicates the flow to 2D-QSI criticality and provides with Eq.(5) an estimate for the oxygen isotope effect on d_s, namely $\Delta d_s/d_s = 3.3(4)\%$.

isotope exchange are not independent, but related by

$$\frac{\Delta T_c}{T_c} = \frac{\Delta d_s}{d_s} + \frac{\Delta\left(1/\lambda_{ab}^2\left(0\right)\right)}{\left(1/\lambda_{ab}^2\left(0\right)\right)} = \frac{\Delta d_s}{d_s} - 2\frac{\Delta\left(\lambda_{ab}\left(0\right)\right)}{\lambda_{ab}\left(0\right)}. \tag{5}$$

In particular, for the oxygen isotope effect (^{16}O vs. ^{18}O) of a physical quantity X the relative isotope shift is defined as $\Delta X/X = (^{18}X - ^{16}X)/^{18}X$. In Fig.4 we show the data for the oxygen isotope effect in $La_{2-x}Sr_xCuO_4$[37, 38], $Y_{1-x}Pr_xBa_2Cu_3O_{7-\delta}$[38, 39, 40] and $YBa_2Cu_3O_{7-\delta}$[38, 41], extending from the underdoped to the optimally doped regime, in terms of $\Delta\left(\lambda_{ab}\left(0\right)\right)/\ \lambda_{ab}\left(0\right)$ versus $\Delta T_c/T_c$. It is evident that there is a correlation between the isotope effect on T_c and $\lambda_{ab}\left(0\right)$ which appears to be universal for all cuprate families. Indeed, the solid line indicates the flow to the 2D-QSI transition and provides with Eq.(5) an estimate for the oxygen isotope effect on d_s, namely $\Delta d_s/d_s = 3.3(4)\%$. Approaching optimum doping, this contribution renders the isotope effect on T_c considerably smaller than that on $\lambda_{ab}\left(0\right)$. As shown in Fig.5, even in nearly optimally doped $YBa_2Cu_3O_{7-\delta}$, where $\Delta T_c/T_c = -0.26(5)\%$, a substantial isotope effect on the in-plane penetration depth, $\Delta\lambda_{ab}\left(0\right)/\lambda_{ab}\left(0\right) = -2.8(1.0)\%$, has been established by direct observation, using the novel low-energy muon-spin rotation technique[41]. Note that these findings have been obtained using various experimental techniques on powders, thin films and single crystals.

Since upon oxygen isotope exchange the lattice parameters remain essentially unaffected[42, 43], the substantial isotope effect on the in-plane penetration depth uncovers the coupling between local lattice distortions and superfluidity and the failure of the Migdal-Eliashberg (ME) treatment of the electron-phonon interaction, predicting, $1/\lambda^2\left(0\right)$, to be independent of the ionic masses[44]. Evidence for this coupling emerges from the oxygen isotope effect on d_s, the thickness of the superconducting sheets, upon isotope exchange, while the lattice parameters remain unaffected. Indeed, the relative shift, $\Delta d_s/d_s \approx 3.3(4)\%$, apparent in Fig.3, implies local distortions of oxygen degrees of freedom, which do not modify the lattice parameters, and are coupled to the superfluid.

Further evidence for this coupling emerges from the isotope effect on the granularity of the cuprates[45, 46]. Recently, it has been shown that the notorious rounding of the superconductor to normal state transition is fully consistent with a finite size effect, revealing that bulk cuprate superconductors break into nearly homogeneous superconducting grains of rather unique extent[14, 45, 46, 47, 48]. Even evidence for their surface and edge contributions to specific heat and penetration depth has been established[49]. A characteristic feature of a finite size effect in the temperature dependence of the in-plane penetration depth λ_{ab} is the occurrence of an inflection point giving rise to an extremum in $d\left(\lambda_{ab}^2\left(T=0\right)/\lambda_{ab}^2\left(T\right)\right)/dT$ at T_p. Here $\lambda_{ab}^2\left(T_p\right)$, T_p and the length L_c of the grains along the c-axis are related by[45, 46, 47, 48, 49]

$$\frac{1}{\lambda_{ab}^2\left(T_p\right)} = \frac{16\pi^3 k_B T_p}{\Phi_0^2 L_c}. \tag{6}$$

Recently we explored the effect of oxygen isotope exchange in $Y_{1-x}Pr_xBa_2Cu_3O_{7-\delta}$ on L_c by means of in-plane

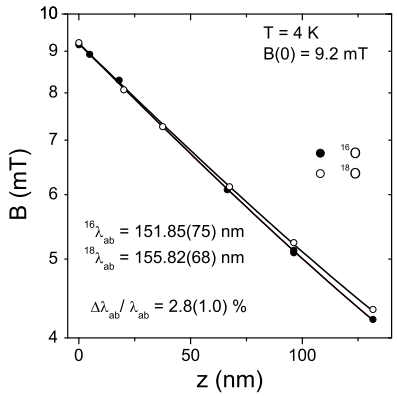

FIG. 5: Magnetic field penetration profiles $B(z)$ for a ^{16}O substituted (closed symbols) and a ^{18}O substituted (open symbols) $YBa_2Cu_3O_{7-\delta}$-film measured in the Meissner state at 4 K and an external field of 9.2 mT, applied parallel to the surface of the film. The data are shown for implantation energies 3, 6, 10, 16, 22, and 29 keV starting from the surface of the sample. Solid curves are best fits to $B(z) = B_0 \cosh[(t-z)/\lambda_{ab}] \cosh(t/\lambda_{ab})$. This is the form of the classical exponential field decay in the Meissner state $B(z) = B_0 \exp(-z/\lambda_{ab})$, modified for a film with thickness $2t$ with flux penetrating from both sides. Taken from Khasanov *et al.*[41]

penetration depth measurements[46]. Note that the shifts are not independent but according to Eq.(6) related by

$$\frac{\Delta L_c}{L_c} = \frac{\Delta T_{p_c}}{T_{p_c}} + \frac{\Delta \lambda_{ab}^2 (T_{p_c})}{\lambda_{ab}^2 (T_{p_c})}. \tag{7}$$

From the resulting estimates, listed in Table I, several observations emerge. First, L_c increases systematically with reduced T_{p_c}. Second, L_c grows with increasing x and upon isotope exchange (^{16}O, ^{18}O). Third, the relative shift of T_{p_c} is very small. This reflects the fact that the change of L_c is essentially due to the superfluid, probed in terms of λ_{ab}^2. Accordingly, $\Delta L_c/L_c \approx \Delta\lambda_{ab}^2/\lambda_{ab}^2$ for $x = 0,\ 0.2$ and 0.3.

x	0	0.2	0.3
$\Delta L_c/L_c$	0.12(5)	0.13(6)	0.16(5)
$\Delta T_{p_c}/T_{p_c}$	-0.000(2)	-0.015(3)	-0.021(5)
$\Delta\lambda_{ab}^2(T_{p_c})/\lambda_{ab}^2(T_{p_c})$	0.11(5)	0.15(6)	0.15(5)
$^{16}T_{p_c}$(K)	89.0(1)	67.0(1)	52.1(1)
$^{16}L_c$(A)	9.7(4)	14.2(7)	19.5(8)
$^{18}T_{p_c}$(K)	89.0(1)	66.0(2)	51.0(2)
$^{18}L_c$(A)	10.9(4)	16.0(7)	22.6(9)

Table I: Finite size estimates for the relative changes of L_c, T_{p_c} and $\lambda_{ab}^2(T_{p_c})$ upon oxygen isotope exchange for $Y_{1-x}Pr_xBa_2Cu_3O_{7-\delta}$[46].

To appreciate the implications of these estimates, we note again that for fixed Pr concentration the lattice parameters remain essentially unaffected [42, 43]. Accordingly, an electronic mechanism, without coupling to local lattice distortions implies $\Delta L_c = 0$. On the contrary, a significant change of L_c upon oxygen exchange requires local lattice distortions involving the oxygen lattice degrees of freedom and implies with Eq.(7) a coupling between these distortions and the superfluid. A glance to Table I shows that the relative change of the grains along the c-axis upon oxygen isotope exchange is significant, ranging from 12 to 16%, while the relative change of the inflection point at T_{p_c}, or the transition temperature, is an order of magnitude smaller. For this reason the significant relative change of L_c at fixed Pr concentration is accompanied by essentially the same relative change of λ_{ab}^2, which probes the superfluid. This uncovers unambiguously the existence and relevance of the coupling between the superfluid and lattice distortions, involving the oxygen lattice degrees of freedom. Furthermore the substantial isotope effect on the in-plane penetration depth at $T = T_{p_c}$ extends the evidence for the failure of the Migdal-Eliashberg (ME) theory of the electron-phonon

interaction, predicting $1/\lambda^2$ to be independent of the ionic masses[44], to finite temperature. Although the majority opinion on the mechanism of superconductivity in the cuprates is that it occurs via a purely electronic mechanism involving spin excitations, and lattice degrees of freedom are supposed to be irrelevant, the relative isotope shifts $\Delta L_c/L_c \approx \Delta\lambda_{ab}^2/^{16}\lambda_{ab}^2 \approx 14\%$ and $\Delta d_s/d_s \approx 3\%$ uncover clearly the existence and relevance of the coupling between the superfluid and local lattice distortions. Recent site-selective oxygen isotope ($^{16}O/^{18}O$) effect measurements of the in-plane penetration depth in $Y_{0.6}Pr_{0.4}Ba_2Cu_3O_{7-\delta}$, using the muon-spin rotation (μSR) technique show that the distortions arise from the oxygen sites within the CuO_2 planes (100 % within error bar)[40]. Potential candidates are then the Cu-O bond-stretching-type modes showing a temperature dependence, which parallels that of the superconductive order parameter[50].

To summarize we observed remarkable consistency between the scaling properties of the experimental data for a variety of cuprates and those characterizing 2D-QSI transitions. The important implication there is that in cuprates a no vanishing transition temperature and superfluid density in the ground state are unalterably linked to a finite anisotropy. Furthermore, the oxygen isotope effect on the in-plane penetration depth and the spatial extent of the superconducting grains revealed the coupling between local lattice distortions and superfluidity, while the lattice parameters remain essentially unaffected. These findings raise serious doubts that 2D models [36], neglecting granularity and local lattice distortions are potential candidates to explain superconductivity in cuprates.

The author is grateful to D. Di Castro, R. Khasanov, K.A. Müller, and J. Roos for very useful comments and suggestions on the subject matter. This work was partially supported by the Swiss National Science Foundation and the NCCR program *Materials with Novel Electronic Properties* (MaNEP) sponsered by the Swiss National Science Foundation.

[1] M. Suzuki and M.Hikita, Phys. Rev. B **44**, 249 (1991).
[2] Y. Nakamura and S. Uchida, Phys. Rev. Phys. Rev. B**47**, 8369 (1993).
[3] Y. Fukuzumi, K. Mizuhashi, K. Takenaka, and S. Uchida, Phys. Rev. Lett. **76**, 684 (1996).
[4] M. Willemin, C. Rossel, J. Hofer, H. Keller, and A. Revcolevschi, Phys. Rev. B **59**, 717 (1999).
[5] T. Kimura, K. Kishio, T. Kobayashi, Y. Nakayama, N. Motohira, K. Kitazawa, and K. Yamafuji, Physica C **192,** 247 (1992).
[6] T. Sasagawa, Y. Togawa, J. Shimoyama, A. Kapitulnik, K. Kitazawa, and K. Kishio, Phys. Rev. B **61**, 1610 (2000).
[7] J. Hofer, T. Schneider, J. M. Singer, M. Willemin, H. Keller, T. Sasagawa, K. Kishio, K. Conder, and J. Karpinski, Phys. Rev. B **62,** 631 (2000).
[8] T. Shibauchi, H. Kitano, K. Uchinokura, A. Maeda, T. Kimura, and K. Kishio, Phys. Rev. Lett. **72**, 2263 (1994).
[9] C. Panagopoulos, J. R. Cooper, T. Xiang, Y. S. Wang and C. W. Chu, Phys. Rev. B **61**, 3808 (2000).
[10] J. L. Tallon, C. Bernhard, H. Shaked, R. L. Hitterman, and J. D. Jorgensen, Phys. Rev. B **51**, 12911 (1995).
[11] M. R. Presland, J. L. Tallon, R. G. Buckley, R. S. Liu, and N. E. Flower, Physica C **176**, 95 (1991).
[12] N. Momono, M. Ido, T. Nakano, M. Oda, Y. Okajima, and K. Yamaya, Physica C **233**, 395 (1994).
[13] T. Schneider, Acta Physica Polonica A **91,** 203 (1997).
[14] T. Schneider and J. M. Singer, *Phase Transition Approach To High Temperature Superconductivity*, Imperial College Press, London, 2000.
[15] T. Schneider and J. M. Singer, J. of Superconductivity **13**, 789 (2000).
[16] T. Schneider and H. Keller, Phys. Rev. Lett. **86**, 4899 (2001).
[17] T. Schneider, Physica B **326**, 289 (2003).
[18] T. Schneider, cond-mat/0204236.
[19] L. Onsager, Phys. Rev. **65**, 117 (1944).
[20] J. Hofer, J. Karpinski, M. Willemin, G.I. Meijer, E.M. Kopnin, R. Molinski, H. Schwer, C. Rossel, and H. Keller, Physica C **297**, 103 (1998).
[21] G. Xiao, M. Z. Cieplak, J. Q. Xiao, and C. L. Chien, Phys. Rev. B **42**, 8752 (1990).
[22] J. M. Tarascon *et al.*, Phys. Rev. B **42**, 218 (1990).
[23] S. Watauchi, H. Ikuta, H. Kobayashi, J. Shimoyama, and K. Kishio, Phys. Rev. B **64**, 64520 (2001).
[24] T. R. Chien, W. R. Datars, B. W. Veal, A. P. Paulikas, P. Kostic, Chun Gu, and Y. Jiang, Physica C **229**, 273 (1994).
[25] T. R. Chien, W. R. Datars, M. D. Lan, J. Z. Liu, and R. N. Shelton, Phys. Rev. B **49**, 1342 (1994).
[26] T. R. Chien and W. R. DatarsJ. Z. Liu, M. D. Lan, and R. N. Shelton, Physica C **221**, 428 (1994).
[27] X. F. Sun, X. Zhao, X.-G. Li, and H. C. Ku, Phys. Rev. B **59**, 8978 (1999).
[28] C. Panagopoulos, J. R. Cooper, N. Athanassopoulou, and J. Chrosch, Phys. Rev. B **54**, 12721 (1996).
[29] P. A. Crowell, F. W. van Keuls, and J. R. Reppy, Phys. Rev. B **55**, 12620 (1997).
[30] Y. Uemura *et al.*, Phys. Rev. Lett. **62**, 2317 (1989).
[31] T. Schneider, Phys. Rev. B **67**, 134514 (2003).
[32] M. P. A. Fisher, G. Grinstein, and S. M. Girvin, Phys. Rev. Lett. **64**, 587 (1990.

[33] Min-Chul Cha, M. P. A. Fisher, M. Wallin, and A. P. Young, Phys. Rev. B **44**, 6883 (1991).
[34] I. F. Herbut, Phys. Rev. B **6**, 14723 (2000).
[35] A. Hosseini, The anisotropic microwave electrodynamics of YBCO, Ph.D. Thesis, University of British Columbia (2002).
[36] P. W. Anderson, P. A. Lee, M. Randeria, T. M. Rice, N. Trivedi, and F. C. Zhang, cond-mat/0311467.
[37] J. Hofer, K. Conder, T. Sasagawa, Guo-meng Zhao, M. Willemin, H. Keller, and K. Kishio, Phys. Rev. Lett. **84**, 4192 (2000).
[38] R. Khasanov, Studies of the oxygen-isotope effect on the magnetic field penetration depth in cuprate superconductors, Ph.D. Thesis, University of Zürich (2003).
[39] R. Khasanov, A. Shengelaya, K. Conder, E. Morenzoni, I. M. Savic, and H Keller, J. Phys.: Condens. Matter **15**, L17 (2003).
[40] R. Khasanov, A. Shengelaya, E. Morenzoni, M. Angst, K. Conder, I. M. Savic, D. Lampakis, E. Liarokapis, A. Tatsi, and H. Keller, Phys. Rev. B **68**, 220506(R) (2003).
[41] R. Khasanov, D. G. Eshchenko, H. Luetkens, E. Morenzoni, T. Prokscha, A. Suter, N. Garifianov, M. Mali, J. Roos, K. Conder, and H. Keller, Phys. Rev. Lett. (2004), in press.
[42] F. Raffa, T. Ohno, M. Mali, J. Roos, D. Brinkmann, K. Conder, and M. Eremin, Phys. Rev. Lett. **81**, 5912 (1998).
[43] K. Conder, Mater. Sci. Eng., R **32**, 41 (2001).
[44] A.B. Migdal, Zh. Eksp. Teor. Fiz. **34**, 1438 (1958) [Sov.Phys. JETP **7**, 996 (1958)]; G. M. Eliashberg, Zh. Eksp. Teor. Fiz. **38**, 966 (1960) [Sov.Phys. JETP **11**, 696 (1960)].
[45] T. Schneider, cond-mat/0308595.
[46] T. Schneider, R. Khasanov, K. Conder, and H Keller, J. Phys. Condens: Matter **15**, L763 (2003).
[47] T. Schneider, Journal of Superconductivity, **17**, 41 (2004).
[48] T. Schneider and D. Di Castro, Phys. Rev. B **69**, 024502 (2004).
[49] T. Schneider, this volume.
[50] J.-H. Chung, T. Egami, R. J. Mc Queeney, M. Yethiraj, M. Arai, T. Yokoo, Y. Petrov, H. A. Mook, Y. Endoh, S. Tajima, C. Frost, and F. Dogan, Phys. Rev. B **67**, 014517 (2003).